Nanoscale

PAPER

View Article Online
View Journal | View Issue

Cite this: *Nanoscale*, 2020, **12**, 610

Skin irritation potential of graphene-based materials using a non-animal test†

Laura Fusco, [a] Marina Garrido, [a] Cristina Martín, [b,c] Silvio Sosa, [d] Cristina Ponti, [d] Alba Centeno, [e] Beatriz Alonso, [e] Amaia Zurutuza, [e] Ester Vázquez, [b,c] Aurelia Tubaro, [d] Maurizio Prato [a,f,g] and Marco Pelin *[d]

Besides inhalation, skin contact may be considered one of the most relevant exposure routes to graphene-based materials (GBMs). However, very few data on the cutaneous toxicity of these materials are available, so far. This study is focused on skin irritation potential of a panel of GBMs: few-layer graphene (FLG), exfoliated by ball milling of graphite, FLG exfoliated by ultrasonication using sodium dodecyl sulfate (FLG-SDS) or sodium dodecylbenzenesulfonate (FLG-SDBS), CVD-graphene, obtained by chemical vapor deposition, graphene oxide (GO) and reduced GO (rGO). Skin irritation was assessed using the SkinEthic™ Reconstructed human Epidermis (RhE), following the Organisation for Economic Co-operation and Development (OECD) Test Guideline (TG) 439. Even though not validated for nanomaterials, the OCED TG 439 turned out to be applicable also for GBM testing, since no interference with the methylthiazolyldiphenyl-tetrazolium bromide (MTT) reduction, used as a final readout, was found. Furthermore, direct epidermal exposure to powdered GBMs mimics the actual human exposure, avoiding interference by the cell culture medium (protein corona formation). Only GBMs prepared with irritant surfactants (FLG-SDS and FLG-SDBS), but not the others, reduced RhE viability at levels lower than those predicting skin irritation (≤50%), suggesting irritant properties. This result was further confirmed by measuring cytokine (IL-1α, IL-6 and IL-8) release by GBM-treated RhE and by histological analysis as additional readouts to implement the guideline. On the whole, these results demonstrate that GBMs prepared with non-irritant exfoliation agents do not induce skin irritation after a single acute exposure.

Received 8th August 2019,
Accepted 8th November 2019

DOI: 10.1039/c9nr06815e

rsc.li/nanoscale

Introduction

Skin represents the major barrier between the human body and environment. Its anatomical structure guarantees protection against external factors, including physical, chemical, and biological agents. An emerging area of concern is represented by skin exposure to manufactured nanomaterials, including metal nanoparticles (*i.e.* TiO_2NPs, AgNPs, AuNPs, *etc.*), nano-

[a]*Department of Chemical and Pharmaceutical Sciences, University of Trieste, Via Giorgieri 1, 34127 Trieste, Italy. E-mail: lfusco@units.it, mgarrido@units.it*
[b]*Instituto Regional de Investigación Científica Aplicada (IRICA), 13071 Ciudad Real, Spain. E-mail: cristina.martin.jimenez89@gmail.com*
[c]*Departamento de Química Orgánica, Facultad de Ciencias y Tecnologías Químicas, Universidad de Castilla-La Mancha (UCLM), 7 13071 Ciudad Real, Spain. E-mail: Ester.Vazquez@uclm.es*
[d]*Department of Life Sciences, University of Trieste, Via Valerio 6, 34127 Trieste, Italy. E-mail: ssosa@units.it, cponti@units.it, mpelin@units.it, tubaro@units.it; Tel: +39040558888620*
[e]*Graphenea, Paseo Mikeletegi 83, Donostia-San Sebastián, 20009, Spain. E-mail: a.centeno@graphenea.com, b.alonso@graphenea.com, a.zurutuza@graphenea.com*
[f]*Carbon Nanobiotechnology Laboratory CIC BiomaGUNE, Paseo de Miramón 182, Donostia-San Sebastián, 20009, Spain. E-mail: prato@units.it*
[g]*Basque Foundation for Science (IKERBASQUE), Bilbao, 48013, Spain*

†Electronic supplementary information (ESI) available: Supplementary Fig. S1. Characterization of disks of CVD-graphene monolayers by optical microscopy (A) and Raman spectroscopy (B). Supplementary Fig. S2. Assessment of technical proficiency on RhE, testing the ten Proficiency substances (PS) according to the OECD TG 431. The table reports the % of RhE viability after PS exposure following the SkinEthic™ Skin Irritation Test-[42bis] and are the mean ± SE of three independent experiments. Irritancy classification was defined on the basis of the threshold given by the OCED TG 439. Supplementary Fig. S3. TGA analyses for the starting graphite, FLG, FLG-SDS and FLG-SDBS (A) and for GO and rGO materials (B). Supplementary Fig. S4. HRTEM picture of FLG. Supplementary Fig. S5. Total reflection X-Ray fluorescence (TXRF) of FLG. Supplementary Fig. S6. XRD analysis of GO (A) and rGO (B). Supplementary Fig. S7. Representative TEM images of GO (A) and rGO (B). Supplementary Fig. S8. MTT interference with GBMs-exposed RhE media. RhE tissues were exposed to GBMs for 42 minutes followed by 42 hours post-incubation without the materials. After treatment, RhE media were collected and 100 μL of each was exposed to 10 μL of MTT reagent (5 mg mL^{-1}) for 3 hours at 37 °C and the absorbance read at 570 nm. As a comparison, 100 μL of the same RhE media were exposed to 10 μL of the WST-8 reagent for 3 hours at 37 °C and the absorbance read at 450 nm. Results are the mean ± SE of three independent experiments. See DOI: 10.1039/c9nr06815e

structured hydrogels and polymers or carbon-based nanomaterials (*i.e.* carbon nanotubes, fullerenes, carbon-quantum dots, *etc.*). Graphene-based materials (GBMs) represent one of the last discovered members of carbon-based nanomaterials.[1] GBMs, including few-layer graphene (FLG), its oxidative product graphene oxide (GO) and other functionalized graphene materials, have been surrounded by increasing interest and expectations due to their unique physicochemical properties. Indeed, on the basis of their high surface area, extraordinary electrical and thermal conductivity and strong mechanical strength, GBMs are promising nanotools for a wide range of possible applications in the fields of nanoelectronics and energy technology, biosensoristic field and biomedicine.[2] Given these properties, an active field of research is represented by the investigation of GBM applications at the skin level, mainly as artificial and electronic skin, wound healing dressings and skin sensors.[3,4] Considering these promising applications, the cutaneous exposure route to GBMs can be assumed as one of the most important ones in the actual scenario. However, the major risk for human health posed by GBMs is currently related to their occupational exposure rather than to an extensive exposure by consumers.[5] Actually, during GBM industrial or laboratory scale production, skin may be considered as one of the main involved exposure routes, after inhalation.[6,7] Moreover, it has to be considered that around 90% of skin diseases related to the occupational settings are represented by irritant and allergic contact dermatitis.[8]

However, despite the importance of skin exposure and the dermotoxic potential of GBMs, very limited data on the cutaneous toxicity of these materials are currently available. Only few *in vitro* data regarding the effects on skin fibroblasts[9] and keratinocytes[10–13] are available, so far. In HaCaT skin keratinocytes, we previously demonstrated that FLG and GO reduced cell viability after interaction with plasma membrane.[11] The effect was significant after exposure times as long as 72 hours at concentrations higher than 1–10 μg mL^{-1}, involving a reactive oxygen species (ROS)-dependent mitochondrial dysfunction, driven by the activation of flavon-based oxidative enzymes.[12]

Hence, considering the potential toxicity of GBMs at the cutaneous level, this study investigates skin irritation properties of a panel of different materials, including FLG, obtained by different procedures, disks of CVD-graphene monolayers, obtained by chemical vapor deposition, GO and its chemically reduced form rGO. Since no specific guidelines for skin testing of nanomaterials are currently available, a specific guideline given by the Organisation for Economic Co-operation and Development (OECD) for *in vitro* testing of chemicals at the skin level was followed. As a first step, the feasibility to apply the OECD guideline to test also a particular class of nanomaterials, such as GBMs, was evaluated. In addition, to implement the OECD guideline procedure for skin irritation, epidermal samples exposed to GBMs were subjected also to histological analysis and the release of selected pro-inflammatory cytokines was also determined.

Experimental

Materials and reagents

FLG was obtained by ball-milling under solvent-free conditions, as a powder easily dispersible in culture media.[14–16] FLG-SDS and FLG-SDBS were prepared by ultrasonication using sodium dodecyl sulfate (SDS) or sodium dodecylbenzenesulfonate (SDBS), respectively. GO (batch #GOB067) and rGO (batch #rGOPB010) were kindly supplied by Graphenea (San Sebastián, Spain).

Disks of CVD graphene monolayers were supplied by Graphenea (San Sebastián, Spain). Graphene was grown by Chemical Vapour Deposition (CVD) on a copper foil catalyst. After growth, a sample of graphene grown on copper foil (5 × 5 cm^2 size) was spin-coated with 80 nm of 495 K PMMA (polymethyl methacrylate). The stack was laminated in a 50 μm thick PMMA laminate at 150 °C using a pressure of 0.5 mbar. After this, the copper was properly etched in a ferric cloride ($FeCl_3$) containing solution and cleaned several times with distilled water and HCl 10 wt% solution. Once the graphene film was cleaned, the square laminate was cut in small disks of 6 mm^2 for testing. Disks of CVD-graphene monolayers were analyzed by optical microscopy using an Eclipse LV 100ND microscope and Raman spectroscopy (WiTec Confocal Raman Microscope) with a 532 nm laser wavelength (ESI Fig. S1†).

Graphite flakes (particle size = +100 mesh), sodium dodecyl sulfate (SDS) and sodium dodecyl-benzenesulfonate (SDBS) used to obtain FLG-SDS and FLG-SDBS were purchased from Sigma-Aldrich (Milan, Italy) and were used without further purification. For the preparation of FLG by ball-milling techniques, SP-1 graphite powder was purchased from Bay Carbon, Inc. (Bay City, MI, USA) and melamine from Sigma-Aldrich (Madrid, Spain).

Preparation of FLG, FLG-SDS and FLG-SDBS

Exfoliation with melamine (FLG). A mixture of 7.5 mg of graphite and 22.5 mg of melamine (1,3,5-triazine-2,4,6-triamine) was ball-milled at 100 rpm for 30 minutes using a Retsch PM 100 planetary mill under an air atmosphere. The resulting solid mixture was dispersed in 20 mL of water and sonicated for 1 min to produce a dark suspension. Melamine was afterwards eliminated by dialysis. Some precipitate, consisting of poorly exfoliated graphite, was removed from the liquid fraction after stabilization for 5 days. The resulting FLG water dispersions were lyophilized and the final graphene powder was thoroughly characterized.[17]

Exfoliation with SDS (FLG-SDS). One gram of graphite was added to 200 mL of SDS/Milli-Q water solution (0.05 mg mL^{-1}). Then, the dispersion was sonicated for 2 hours and subsequently was centrifuged for 45 minutes at 500 rpm. Finally, the supernatant was collected and lyophilized, affording the final FLG-SDS powder.

Exfoliation with SDBS (FLG-SDBS). One gram of graphite was added to 200 mL of SDBS/Milli-Q water solution (0.05 mg mL^{-1}). Then, the dispersion was sonicated for 2 hours and subsequently was centrifuged for 45 minutes at

500 rpm. Finally, the supernatant was collected and lyophilized, affording the final FLG-SDBS powder.

Characterization techniques

Raman spectra were recorded on a Renishaw inVia Raman Microscope at room temperature using an exciting laser source of 532 nm. Raman samples were measured in solid state under ambient conditions. Transmission electron microscopy (TEM) micrographs were obtained using a Philips EM208 TEM and RADIUS 2.0 software (EMSIS GmbH, Muenster, Germany). The samples were dispersed in Milli-Q water and dropped onto a lacey carbon copper grid (300 mesh); the solvent was removed at room temperature. High-Resolution Transmission Electron Microscopy (HRTEM) was performed in a JEOL 2100. Thermogravimetric analyses (TGA) were performed with a TGA Q500 (TA Instruments) under a N_2 atmosphere. The sample was introduced inside a platinum crucible and equilibrated at 100 °C followed by a 10 °C min^{-1} ramp between 100 and 800 °C. Elemental analysis was performed with a LECO CHNS-932 analyzer, completely burning the sample with four doses of oxygen, and quantifying the released gases by thermal conductivity. Total reflection X-Ray fluorescence (TXRF) measurements of FLG and GO were performed using a Bruker-S2 PicoFox TXRF spectrometer.

Skin irritation

SkinEthic™ Reconstructed Human Epidermis (RhE) model. Skin irritation was evaluated on the SkinEthic™ Reconstructed Human Epidermis (RhE), a fully differentiated three-dimensional epidermal tissue constituted of normal human keratinocytes in a chemically defined medium grown at the air–liquid interface. The SkinEthic™ RhE model was purchased from Episkin (Lyon, France) and checked for quality control criteria (mean optical density, O.D., of 3 negative controls = 1.37 ± 0.04 and mean viability of 3 positive controls, 5% SDS = 2.1 ± 0.4%), before being used for the experiments. Technical proficiency was assessed testing the ten Proficiency substances according to OECD TG 439 (ESI Fig. S2†).

SkinEthic™ Skin Irritation Test^{-42bis}. Skin irritation induced by GBMs was evaluated on the SkinEthic™ RhE model following the skin Irritation Test^{-42bis}, a test compliant with the OECD Test Guideline (TG) No. 439 for testing of chemicals, due to the lack of specific OECD guidelines for nanomaterials.

As reported by OECD TG 439, RhE tissues (0.5 cm^2, at day 17) were topically exposed to 16 mg FLG, FLG-SDS, FLG-SDBS, GO or rGO (32 mg cm^{-2}) in triplicate for 42 min at room temperature (RT), after adding 10 μL of distilled water on the RhE surface. For CVD-graphene, each disk was added above the epidermis surface. As negative (vehicle) and positive controls, tissues were exposed to phosphate buffered saline (PBS) or 5% w/v SDS, respectively. As an additional positive control, RhE was exposed also to 5% w/v SDBS. RhE tissues were then washed 25 times with 1 mL PBS and transferred in a 6-well plate with 2 mL growth medium. After 42 h post-incubation at 37 °C, 5% CO_2, tissue viability was assessed by the MTT reduction assay: RhE samples were transferred in a 24-well plate containing 300 μL of MTT solution (1 mg mL^{-1}) and incubated for 3 h at 37 °C, 5% CO_2. Formazan crystals were then extracted from the tissue adding isopropanol (1.5 mL per well, for 2 h at RT). Tissue viability is reported as % of negative controls (vehicle), measuring the O.D. of each isopropanol extract in triplicate at 570 nm by using an Automated Microplate Reader EL 311s (Bio-Tek Instruments; Winooski, VT, USA). Results are the mean ± SE of three independent experiments.

Evaluation of GBM-induced interference

Since GBMs have been reported to interact with the MTT reagent, giving its possible unspecific reduction,[9] as preliminary experiments, "killed" RhE tissues were used to evaluate the non-specific reduction of MTT. As reported by OECD TG 439, "killed" RhE tissues were obtained by freezing treatment at −80 °C for 48 h and further processed for GBM treatment and MTT assay as reported above. Data are reported as optical density (O.D.) measured at 570 nm and are the mean ± SE of 3 independent experiments.

To further exclude interference, tissue media (200 μL) were collected from RhE after GBM treatment and further exposed to the MTT reagent for 3 h at 37 °C, as reported above. To confirm the results, 200 μL of tissue media were exposed for 3 h at 37 °C to 20 μL of 2-(2-methoxy-4-nitrophenyl)-3-(4-nitrophenyl)-5-(2,4-disulfophenyl)-2*H*-tetrazolium (WST-8) that is not reported to have any unspecific interaction with GBMs.[9] Absorbance was subsequently read at 450 nm by using an Automated Microplate Reader EL 311s (Bio-Tek Instruments; Winooski, VT, USA). Data are reported as O.D. measured at 450 nm and are the mean ± SE of 3 independent experiments.

Histological analysis

Immediately after treatment (42 min exposure to GBMs and/or positive controls followed by 42 h post-exposure), RhE specimens were collected from each insert and fixed in 10% (v/v) neutral buffered formaldehyde. RhE specimens were then dehydrated, embedded in paraffin and longitudinally sectioned to avoid any passive transport of GBMs deposited on the epidermis surface over the different layers. Sections were then stained with hematoxylin/eosin and analyzed under the Axio Scope A1 optical microscope (Zeiss, Milan, Italy) and microphotographs were collected through the Axiocam 503 color digital camera (Zeiss, Milan, Italy) using the Zen2 software, with a 40× magnification. Images were collected from 6 different samples.

Cytokine quantitation

Immediately after treatment (42 min exposure to GBMs and/or positive controls followed by 42 h post-exposure), culture media were collected and stored at −80 °C. A panel of pro-inflammatory cytokines (interleukin, IL, -1α, -6 and -8) was evaluated by specific sandwich ELISAs from Diaclone (Tema Ricerca, Milan, Italy), following the manufacturer's instructions. Results are expressed as pg mL^{-1} of cytokines released in the media and are the mean ± SE of three independent experiments.

Statistical analysis

For skin irritation (OECD TG 439), results are expressed as % of tissue viability with respect to vehicle controls and are the mean ± SE of three independent experiments. As a threshold given by OECD TG 439, viability ≤50% defines an irritant compound.

Statistical analysis was performed by a one-way ANOVA followed by Bonferroni's post test (GraphPad Prism version 6.00) and statistical significance was considered for $p < 0.05$.

Results

Physico-chemical characterization of GBMs

FLG. FLG was characterized by Raman spectroscopy, TEM, TGA, TXRF and elemental analysis. The TGA curve displayed a weight loss of 6.4% at 600 °C, indicating the low quantity of oxygen groups generated by the exfoliation process (ESI Fig. S3†). Elemental analysis showed average values of 94.93 ± 0.28% C, 0.55 ± 0.02% H, 0.54 ± 0.02% N (Table 1). The oxygen content, less than 3.7%, is compatible with the weight loss at 600 °C observed by TGA, and the traces of melamine resulted in only 0.81%.

The average Raman spectrum of FLG (40 spectra) showed the two most intense peaks of graphene, the G band and the 2D peak, which appear at around ~1580 cm^{-1} and ~2700 cm^{-1}, respectively (Fig. 1A). The average $I(2D)/I(G)$ ratio is 0.45, proving the samples to be few-layer graphene, usually assigned for $I(2D)/I(G) < 1$.[18,19] In fact, only 4 layers were calculated for FLG.[20] When graphene is affected by defects, a peak appears at around 1345 cm^{-1} (D band). In this case, the average spectrum of FLG shows a $I(D)/I(G)$ ratio about 0.37, corroborating the low level of defects which are attributed to the edges of the micrometer flakes.[21]

The lateral dimension of FLG was estimated by TEM analysis after the evaluation of at least 100 different sheets. The

Table 1 Physicochemical properties of FLG, FLG-SDS, FLG-SDBS, GO and rGO

GBMs	Elemental Analysis ± SD (%)					TGA weight loss[a] (%)	Lateral dimension ± SD (nm)	Lateral dimension distribution (nm)	No. layers
	C	H	N	S	O				
FLG	94.93 ± 0.28	0.55 ± 0.02	0.54 ± 0.02	0.32 ± 0.03	<3.7	6	171 ± 147[b]	50–600[b]	4
FLG-SDS	56.65 ± 0.07	2.31 ± 0.05	0.39 ± 0.12	4.06 ± 0.12	<36.6	22	917 ± 389[b]	360–2200[b]	5
FLG-SDBS	52.75 ± 0.19	2.70 ± 0.04	0.13 ± 0.02	3.54 ± 0.12	<40.9	23	1097 ± 568[b]	400–4500[b]	5
GO	59.40 ± 0.10	1.40 ± 0.10	0.07 ± 0.02	2.50 ± 0.10	<36.6	46	15 100 ± 400[c]	6000–30000[c]	6[d]
rGO	81.30 ± 0.20	0.82 ± 0.02	0.21 ± 0.01	nd	<17.7	17	5500 ± 200[c]	3000–11000[c]	2[d]

[a] Values determined at 600 °C. [b] Values determined by TEM on at least 100 sheets. [c] D_{50} values determined by laser diffraction in the GO slurry and rGO powder. [d] Calculated by XRD in GO dry film and rGO powder.

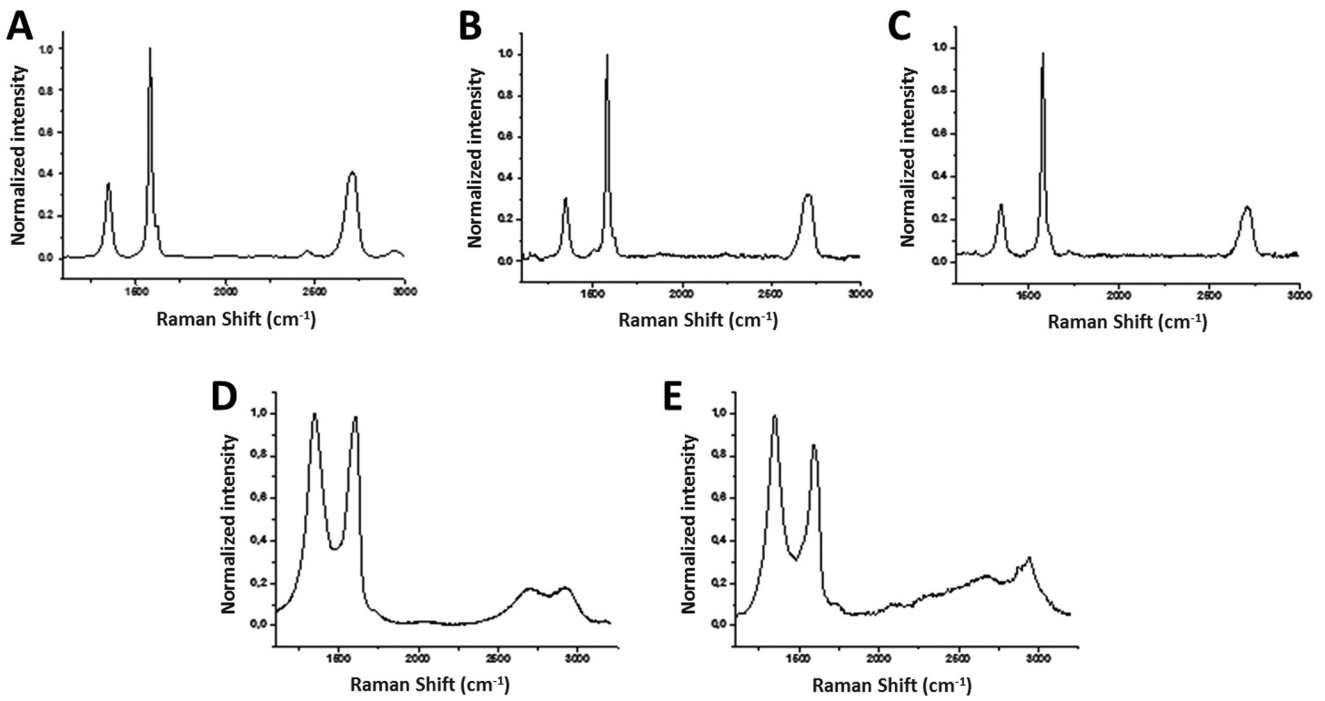

Fig. 1 Raman spectra (λ_{exc} = 532 nm) of FLG (A), FLG-SDS (B), FLG-SDBS (C), GO (D) and rGO (E).

lateral size distribution was located mainly between 50 and 600 nm with an average lateral dimension of 171 ± 147 nm (Fig. 2A). A representative TEM image of the obtained FLG is shown in Fig. 2B. The number of layers was also corroborated by HRTEM analysis (ESI Fig. S4†).

Finally, since a stainless-steel flask is used during the ball-milling process, TXRF was performed to ensure the absence of metals, especially Fe, in the FLG sample, revealing a Fe concentration of only 0.074 mg L^{-1} (ESI Fig. S5†).

FLG-SDS and FLG-SDBS. FLG-SDS and FLG-SDBS were characterized by Raman spectroscopy, TEM, TGA and elemental analysis. Raman analyses were performed to corroborate the successful exfoliation of graphite in the presence of both surfactants (Fig. 1B and C). The Raman spectrum of graphitic

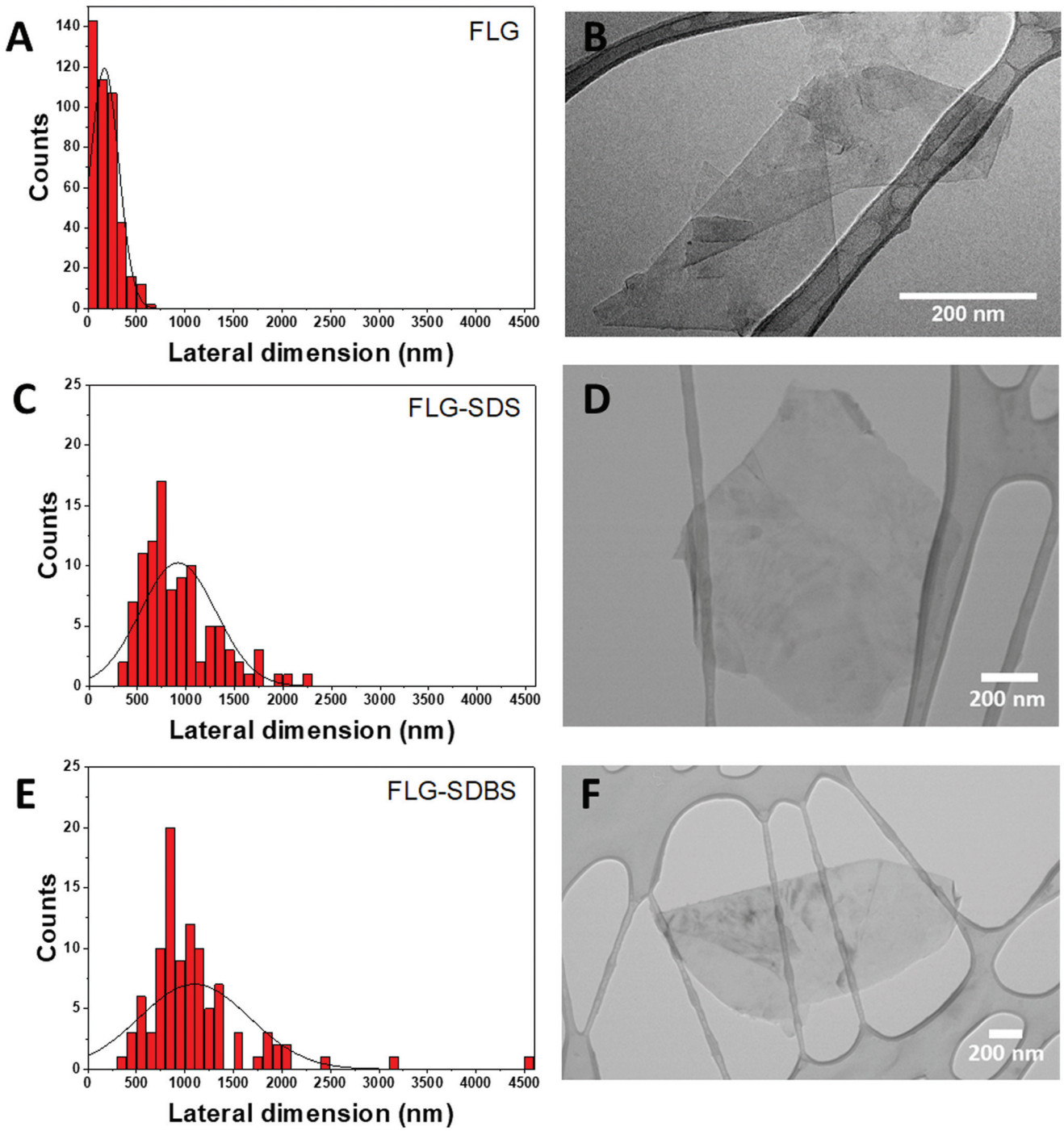

Fig. 2 Lateral dimension distribution from TEM images (A, C, and E) and representative TEM images (B, D, and F) of FLG (A and B), FLG-SDS (C and D) and FLG-SDBS (E and F).

materials was characterized by three bands: D (~1350 cm^{-1}), G (~1580 cm^{-1}) and 2D (~2700 cm^{-1}). The change of the intensity and position of the 2D band allowed determining the number of layers present after the exfoliation procedure. In this particular case, 5 layers were calculated for both FLG-SDS and FLG-SDBS.[20] Moreover, the $I(D)/I(G)$ ratio allows estimating the number of defects present in the materials, the value of this ratio being 0.31 for the FLG obtained in the presence of SDS and 0.33 in the presence of SDBS.

The lateral dimensions of both materials were estimated by TEM analysis after the evaluation of 100 different sheets for each case. The lateral size distribution was located between 360 and 2200 nm with an average lateral dimension of 917 ± 389 nm for FLG-SDS (Fig. 2C) and between 400 and 4500 nm with an average lateral dimension of 1097 ± 568 nm for FLG-SDBS (Fig. 2E). Representative TEM images of the obtained materials are shown in Fig. 2.

Thermogravimetric analyses (TGA) were performed to determine the quantity of the surfactant present in the exfoliated materials after the lyophilization process (ESI Fig. S3†). As observed in the curves, the starting graphite does not present a significant weight loss (1%). Therefore, the weight loss observed after the exfoliation was due to the presence of both surfactants that interact with the material and allow its exfoliation in water, as well as to the defects created in the graphene flakes during the exfoliation process (TGA weight losses of 22% and 23% for FLG-SDS and FLG-SDBS, respectively, at 600 °C). These values are compatible with the quantity of the surfactant calculated from elemental analysis (36.6 mg of SDS and 38.5 mg of SDBS in 100 mg of the respective obtained materials).

GO and rGO. GO and rGO were characterized by Raman spectroscopy, TEM, TGA and elemental analysis. The average Raman spectrum of GO showed the two characteristic D and G bands, with their maxima located at ~1350 and ~1600 cm^{-1}, respectively (Fig. 1D). Elemental analysis showed average values of 59.40 ± 0.10% C, 1.40 ± 0.10% H, and 0.07 ± 0.02% N (Table 1). At 600 °C, TGA showed a weight loss of 46% (ESI Fig. S3†). The lateral dimension was determined by laser diffraction in the GO slurry: the lateral size distribution was located mainly between 6000 and 30 000 nm with an average lateral dimension of 15 100 ± 400 nm. X-ray diffraction (XRD) analysis performed on a GO dry film (ESI Fig. S6†) revealed 6 layers. Representative TEM images are shown in ESI Fig. S7.†

The average Raman spectrum of rGO showed the two characteristic D and G bands, with their maxima located at ~1350 and ~1590 cm^{-1}, respectively (Fig. 1E). Elemental analysis showed average values of 81.30 ± 0.20% C, 0.82 ± 0.02% H, 0.21 ± 0.01% N (Table 1). At 600 °C, TGA showed a weight loss of 17% (ESI Fig. S3†). The shift to lower frequencies of the G band, the increase of the percentage of carbon in the elemental analysis and the decrease of the weight loss in the TGA confirmed the successful reduction process. The lateral dimension was determined by laser diffraction in rGO powder: the lateral size distribution was located mainly between 3000 and 11 000 nm with an average lateral dimension of 5500 ± 200 nm. XRD analysis performed on rGO powder (ESI Fig. S6†) revealed 2 layers. Representative TEM images are shown in ESI Fig. S7.†

SkinEthic™ Skin Irritation Test[-42bis]

To evaluate the irritation potential of GBMs, a set of experiments was carried out following OECD TG 439, using the SkinEthic™ Skin Irritation Test[-42bis] (42 minutes exposure + 42 hours post-incubation). Briefly, RhE tissues were topically exposed to 16 mg of FLG, FLG-SDS, FLG-SDBS, GO or rGO as powder at the air–liquid interface for 42 minutes followed by 42 h post-incubation without the materials (see materials and methods). Disks of CVD-graphene were topically applied on RhE surfaces for the same exposure time.

As a preliminary set of experiments, the possible interference between GBMs and the MTT reduction was investigated. For MTT-interacting test substances, OECD TG 439 considers the execution of the MTT assay on "killed" RhE tissues after exposure to the test substances, to ensure that the eventual MTT conversion, if any, is given only by the substance. As reported in Fig. 3, none of the GBMs significantly increased O.D. values as compared to untreated controls (vehicle), suggesting that in this model, no unspecific interactions with the MTT reagent can be observed for GBMs. This result was further corroborated by the absence of a significant O.D. increase given by incubation of the MTT reagent with RhE media collected from GBM-treated RhE tissues. As a reference method that does not show any interference with GBMs, WST-8 assay was carried out on RhE media collected from GBM-treated RhE tissues. As expected, also in this case no significant O.D. increase was observed (ESI Fig. S8†).

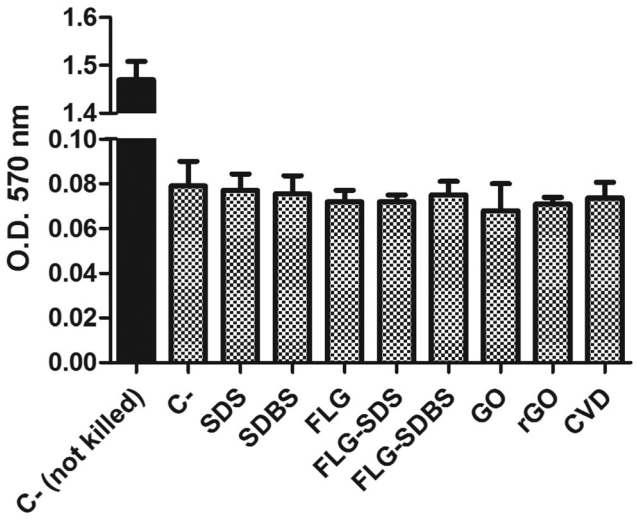

Fig. 3 Interference between GBMs and MTT reagent. According to OECD TG 439, "killed" RhE tissues were exposed to GBMs for 42 minutes exposure + 42 hours post-incubation without the materials and the MTT reduction evaluated in comparison with not killed RhE tissues not exposed to GBMs. Results are presented as optical density (O.D.) measured at 570 nm and are the mean ± SE of 3 independent experiments.

Table 2 Assessment of skin irritation properties of GBMs using the SkinEthic™ Skin Irritation Test-42bis (OCED TG 439)

	Dose	% viability (mean ± SE)	Viability reduction (%)	Irritancy classification
FLG	32 mg cm^{-2}	101 ± 4	−1	NI
FLG-SDS	32 mg cm^{-2}	15 ± 7***	85	I
FLG-SDBS	32 mg cm^{-2}	35 ± 11***	65	I
CVD-graphene	—	96 ± 1	4	NI
GO	32 mg cm^{-2}	96 ± 2	4	NI
rGO	32 mg cm^{-2}	79 ± 4*	21	NI
Positive control (5% SDS in PBS)	32 μL cm^{-2}	3 ± 1***	97	I
Positive control (5% SDBS in PBS)	32 μL cm^{-2}	2 ± 1***	98	I

Results are the mean ± SE of three independent experiments. Irritancy classification was defined on the basis of the threshold given by the OCED TG 439. Statistical differences *vs.* vehicle controls: *, $p < 0.05$; ***, $p < 0.001$ (One-way ANOVA and Bonferroni's post test). NI = non-irritant substance; I = irritant substance.

According to the OECD guidelines, irritancy was assessed by means of tissue viability, measured by the MTT assay. Table 2 shows the results, obtained over 3 independent replicates. In particular, FLG, GO, rGO and CVD-graphene did not reduce RhE viability at levels lower than the threshold given by OECD TG 439 (tissue viability ≤50%) and, therefore, they can be considered as non-irritant materials. In addition, rGO was able to significantly reduce RhE viability by 21% ($p < 0.05$), a level that, however, does not suggest an irritation potential. In contrast, FLG exfoliated with SDS or SDBS significantly reduced RhE viability by 85% and 65%, respectively, levels higher than the threshold for irritation potential given by OECD TG 439, suggesting that these materials can be an irritant for the skin.

The positive control (5% SDS) significantly reduced RhE viability by 97% ($p < 0.001$), indicating that it is an irritant compound. As an additional control, RhE tissues were exposed also to 5% SDBS that significantly reduced RhE viability by 98% ($p < 0.001$).

Considering that some of the FLG materials are obtained by exfoliation with surfactants, such as SDS, the positive control of OECD TG 439, a comparison of the effects induced by FLG-SDS and FLG-SDBS with that induced by FLG was evaluated. RhE viability reductions induced by FLG-SDS (85%) and FLG-SDBS (65%) were significantly higher (p values of 0.0005 and 0.0017, respectively) than that induced by FLG (−1%; Table 3).

Histological analysis

Histological analysis was carried out on hematoxylin/eosin stained RhE specimens (Fig. 4). Panel A of Fig. 4 shows the histological analysis of the negative control: the *stratum corneum* was characteristically dense and the presence of a high number of granules was observed in the *stratum granulosum*. Moreover, nuclei of proliferating keratinocytes of the *stratum spinosum* and *stratum basale* were typically rounded. In contrast, the positive controls SDS (panel B) and SDBS (panel C) presented dramatic morphological alterations typical of skin irritation, with a loss of *stratum corneum* density as well as destruction and partial removal of the *stratum corneum* and *stratum granulosum.* In addition, fragmentation of nuclei of keratinocytes of the *stratum spinosum* and *stratum basale* was observed. For GBMs, loss of the typical density of the *stratum corneum*, to a similar extent of that induced by the positive controls, was observed in RhE exposed to FLG-SDS and FLG-SDBS (panels E–F). Furthermore, morphological alterations, compatible with skin irritation, were observed in the *stratum corneum* and *stratum granulosum* as well as fragmentation of nuclei of keratinocytes of the *stratum spinosum* and *stratum basale*. For the other GBMs, no signs of epidermis irritation or other alterations can be observed. Only slight damage was observed in the outermost layers of the *stratum corneum* of GO-treated epidermis (panel G).

In addition, histological analysis demonstrated the presence of aggregated GBMs (indicated by the arrows; Fig. 4) above the epidermis surfaces in a different fashion depending on the material: (i) small flat agglomerates for FLG materials, appearing larger in FLG-SDS and FLG-SDBS; (ii) larger rounded aggregates for rGO; (iii) absence of material on the epidermis surface for GO and CVD-graphene. Intriguingly, on increasing the magnification of the images (Fig. 5), the presence of small depots of GBMs was observed within the epidermis for all the materials, except for CVD-graphene. In all the cases, these depots were limited to the *stratum corneum* and were far smaller than the aggregates observable above the epidermis surfaces.

Table 3 Comparison between RhE viability reduction (MTT assay) induced by FLG, FLG-SDS and FLG-SDBS using the SkinEthic™ Skin Irritation Test-42bis (OCED TG 439)

	Dose	Viability reduction (%)	p value[a]	Surfactants content[b]
FLG	32 mg cm^{-2}	−1	—	0.8%
FLG-SDS	32 mg cm^{-2}	85	0.0005	36.6%
FLG-SDBS	32 mg cm^{-2}	65	0.0017	38.5%

Results are the mean ± SE of three independent experiments. [a] Statistical differences *vs.* FLG (One-way ANOVA and Bonferroni's post test). [b] Surfactant content (SDS or SDBS) was evaluated by Elemental Analysis, considering the % of N and S in the samples.

Cytokine release

A panel of cytokines (IL-1α, IL-6 and IL-8) was evaluated by specific ELISA assays on RhE media collected after GBM exposure. Fig. 6 shows the amount of the specific cytokines, expressed as pg mL^{-1}, released by RhE after GBM treatment,

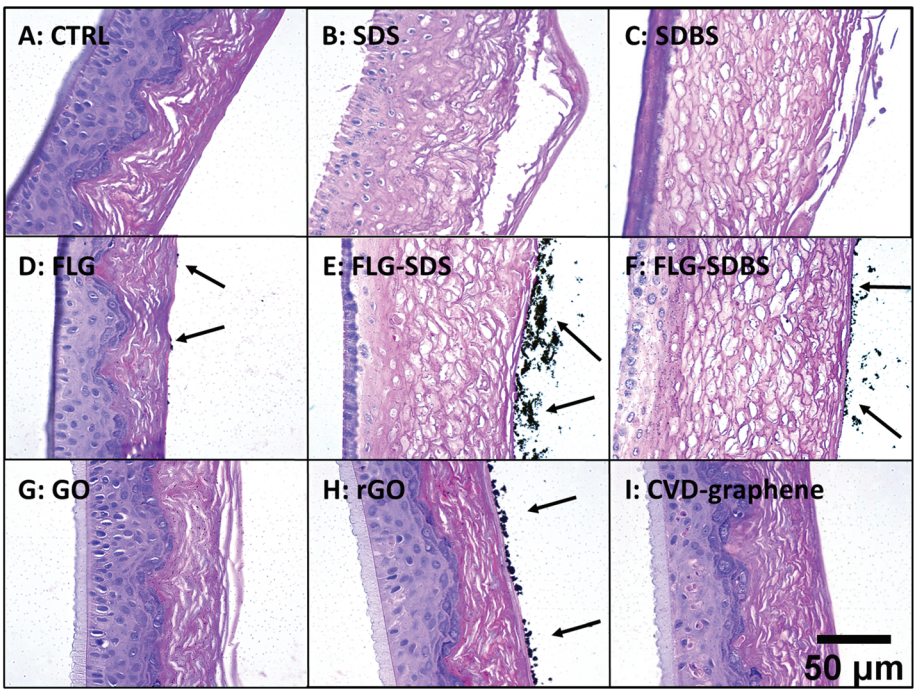

Fig. 4 Histological analysis of RhE exposed to vehicle (A), SDS (B) and SDBS (C) positive controls, FLG (D), FLG-SDS (E), FLG-SDBS (F), GO (G), rGO (H) or CVD (I). After material exposure, RhE specimens were collected, fixed and hematoxylin/eosin stained. Images, representative of 6 different samples, were observed by using an optical microscope. Arrows underline the presence of GBM aggregates and agglomerates above the epidermis surface. Scale bar: 50 μm.

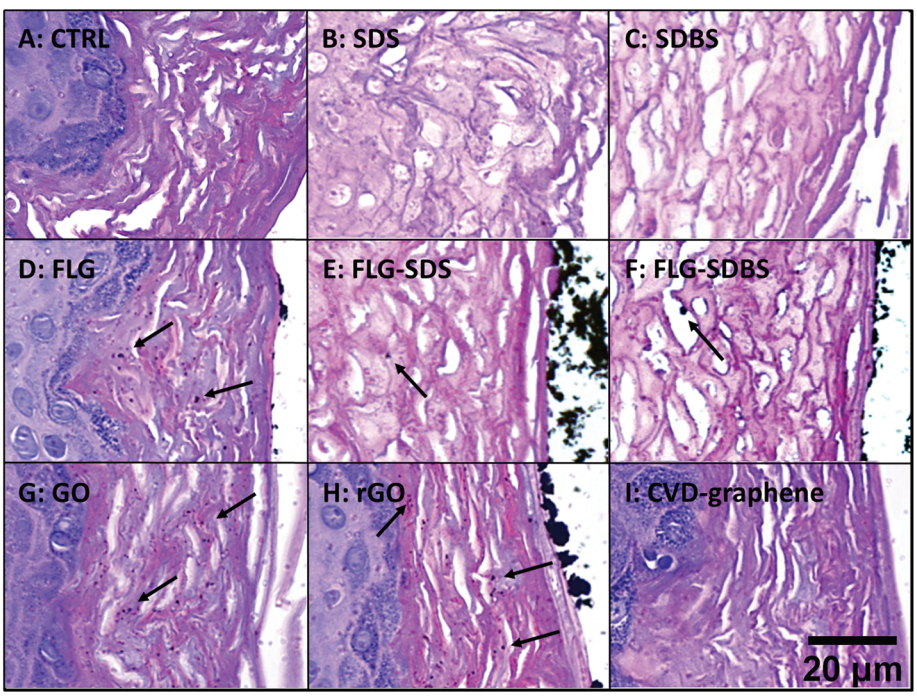

Fig. 5 Presence of GBMs above the epidermis surface and within the *stratum corneum* (shown by arrows) in RhE exposed to vehicle (A), SDS (B) and SDBS (C) positive controls, FLG (D), FLG-SDS (E), FLG-SDBS (F), GO (G), rGO (H) or CVD (I). The image was obtained by an enlargement of Fig. 1. Scale bar: 20 μm.

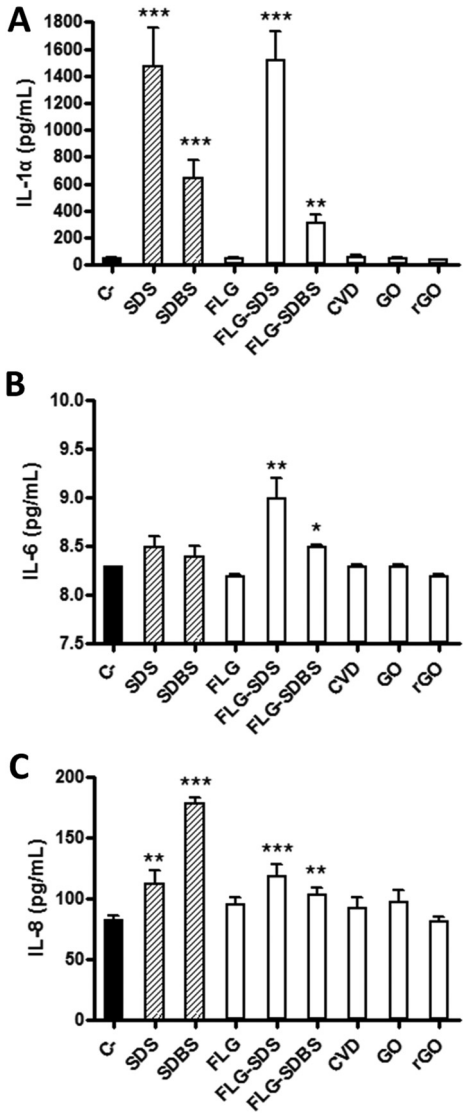

Fig. 6 Cytokine release from RhE exposed to GBMs. After exposure to GBMs, RhE media were collected and IL-1α (A), IL-6 (B) and IL-8 (C) were measured by specific ELISA assays. The data, reported as pg mL^{-1} of cytokines released in the media, are the mean ± SE of three independent experiments. Statistical differences *vs.* negative controls: *, $p < 0.05$; **, $p < 0.01$; ***, $p < 0.001$ (One-way ANOVA and Bonferroni's post test).

in comparison with negative controls and positive controls (RhE exposed to 5% SDS or 5% SDBS).

In particular, considering IL-1α (Fig. 6, panel A), as compared to the negative control (52 pg mL^{-1}), only FLG-SDS and FLG-SDBS were able to significantly increase its release to 1522 pg mL^{-1} (increase of 2826%; $p < 0.001$) and 315 pg mL^{-1} (increase of 505%; $p < 0.01$), respectively. In contrast, the other GBMs did not induce a significant effect with respect to the negative control. The positive controls SDS and SDBS significantly increased the release of IL-1α to 1478 pg mL^{-1} (increase of 2742%; $p < 0.001$) and 645 pg mL^{-1} (increase of 1140%; $p < 0.001$), respectively.

Regarding IL-6 (Fig. 6, panel B), as compared to the negative control (8.2 pg mL^{-1}), only FLG-SDS and FLG-SDBS were able to slightly, but significantly increase its release to 9.0 pg mL^{-1} (increase of 10%; $p < 0.01$) and 8.6 pg mL^{-1} (increases of 5%; $p < 0.05$), respectively. In contrast, the other GBMs as well as the positive controls SDS and SDBS did not induce a significant increase of IL-6 as compared to the negative control.

Also considering IL-8 (Fig. 6, panel C), as compared to the negative control (83 pg mL^{-1}), only FLG-SDS and FLG-SDBS were able to slightly, but significantly increase its release to 119 pg mL^{-1} (increase of 43%; $p < 0.001$) and 104 pg mL^{-1} (increase of 25%; $p < 0.01$), respectively. In contrast, the other GBMs did not induce a significant release with respect to the negative control. The positive controls SDS and SDBS significantly increased the release of IL-8 to 112 pg mL^{-1} (increase of 35%; $p < 0.01$) and 178 pg mL^{-1} (increase of 114%; $p < 0.001$), respectively.

Role of surfactants in the irritation potential of FLG-SDS and FLG-SDBS

To verify the role of surfactant residues in irritation potential of FLG after exfoliation with SDS or SDBS, after the exfoliation procedure the supernatants were filtered under vacuum on a PTFE membrane and washed with Milli-Q water to remove the excess of each surfactant. Both materials were then physicochemically characterized and tested for their skin irritant potential following OECD TG 439, by histological analysis and cytokine release (Fig. 7), as reported above.

"Washed" FLG-SDS and FLG-SDBS were characterized by average lateral dimensions of 500 ± 237 and 495 ± 392 nm, respectively, as assessed by TEM analysis. Raman spectroscopy showed flakes constituted by 6 layers for both materials. The washing procedure significantly reduced the amount of surfactant residue, being equal to 0.22% and 1.90% for FLG-SDS and FLG-SDBS, respectively, as assessed by elemental analysis (Fig. 7A). Following OECD TG 439, the so-obtained materials turned out to be non-irritant, reducing RhE viability at 89% ($p < 0.05$) and 90%, respectively. As confirmatory endpoints, also histological analysis did not show any alteration related to skin irritation (Fig. 7B), as previously observed for the non-irritant FLG exfoliated with melamine (Fig. 4, panel D). Histological analysis also showed the presence of large agglomerates of FLG-SDS and FLG-SDBS above the epidermis surface, as previously shown for the same material before the washing step. In addition, both materials did not induce any significant release of IL-1α, IL-6 and IL-8 as compared to untreated controls (Fig. 7C), confirming the negligible effects of the washed materials on RhE.

Discussion

Recently, GBMs have attracted attention for their extraordinary physicochemical properties, because of a wide range of promising applications in the biomedical and electronic fields. Among them, their potential skin applications, mainly as artificial and electronic skin, wound healing dressings and skin sensors,[3,4] pose a serious concern for the safety of GBMs at the

A

	Elemental Analysis ± SD (%)					Surfactants content[a]	TGA weight loss (%)[b]	Lateral dimension ± SD (nm)[c]	Lateral dimension distribution (nm)[c]	n° layers	Dose (mg/cm²)	% viability (mean ± SE)	Irritancy classification
	C	H	N	S	O								
FLG-SDS (washed)	65.46±0.19	1.05±0.03	0.15±0.01	0.03±0.01	<33	0.22%	6	500±237	150-1400	6	32	89 ± 2*	NI
FLG-SDBS (washed)	59.83±0.18	1.17±0.08	0.05±0.02	0.18±0.01	<38	1.90%	14	495±392	100-2400	6	32	90 ± 3	NI

* Statistical differences *vs* FLG (One-way ANOVA and Bonferroni's post test).
[a] Surfactants content (SDS or SDBS) was evaluated by Elemental Analysis, considering the % of N and S in the samples.
[b] Values determined at 600 °C.
[c] Values determined by TEM on at least 100 sheets.

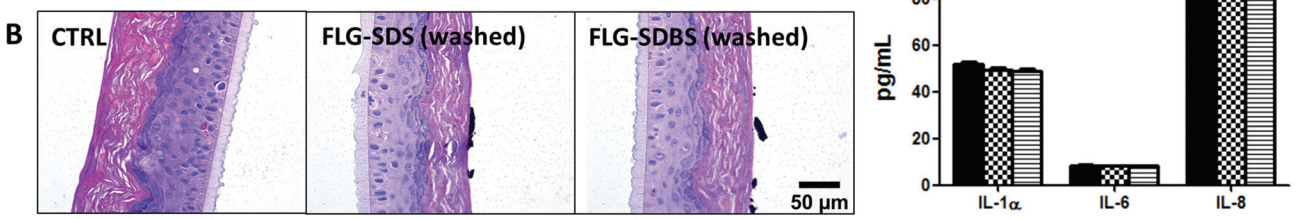

Fig. 7 Irritation potential of "washed" FLG-SDS and FLG-SDBS. Both materials were washed with Milli-Q water after the exfoliation procedure to the obtained materials characterized by very low amounts of surfactant residues. (A) Physicochemical characterization and skin irritation potential of the washed materials, assessed by OECD TG 439. (B) Histological analysis of RhE exposed to untreated controls, FLG-SDS or FLG-SDBS after hematoxylin/eosin staining; scale bar: 50 μm. (C) Release of IL-1α, IL-6 and IL-8 from RhE exposed to FLG-SDS or FLG-SDBS as compared to untreated controls, measured by specific ELISA assays. The data, reported as pg mL^{-1} of cytokines released in the media, are the mean ± SE of three independent experiments.

cutaneous level. The major risk for human health is actually related mainly to occupational exposure to these materials.[5] In this scenario, the cutaneous and inhalation exposures represent the main human routes involved.[6] However, as compared to other GBM exposure routes, the cutaneous one is largely unexplored.[7] In this view, we recently provided *in vitro* data on the effects of different GBMs (FLG and GO) towards human HaCaT skin keratinocytes. On these cells, GBMs exerted a significant cytotoxicity[11] mediated by ROS-dependent mitochondrial damage.[12] However, despite their wide use, HaCaT cells are a simplified *in vitro* model, useful as a first-round screening, also to investigate the mechanism of skin toxicity, but unable to completely predict the relevant toxicity after cutaneous exposure. Indeed, being a proliferating cell line, HaCaT cells fail to recapitulate *in vitro* one of the essential functions of the skin: the barrier function.

Considering the chemical nature of GBMs, in this study we focused on their potential to cause irritant dermatitis, a possible outcome consequent to GBM cutaneous exposure. For decades, the evaluation of skin irritation has been carried out using the Draize rabbit test for all regulatory studies. Due to ethical issues, the *in vitro* EpiSkin™ test method was validated in 2007 by the European Centre for the Validation of Alternative Methods (ECVAM) as a full replacement method for the Draize acute skin irritation test and adopted in OECD TG 439 in 2009. Recently, the SkinEthic™ Reconstructed Human Epidermis (RhE) model has been formally adopted for the regulatory assessment of skin irritation (OECD TG 439). The RhE model is reconstructed starting from normal human skin keratinocytes grown for 17 days in a chemically defined medium. The tissue model consists of a fully differentiated epidermis including the *stratum basale*, *stratum spinosum*, *stratum granulosum* and *stratum corneum*. In this model, a test method compliant with the OCED TG 439, defined 42bis (42 minutes exposure + 42 hours post-incubation), was set up and chosen as the best for its high reproducibility, robustness and predictive capacity.[22] Irritancy prediction is based on the ability of irritant substances to reduce RhE viability (measured by the MTT assay) at levels ≤50% as compared to negative controls.

Since specific OECD guidelines for the prediction of skin irritation caused by nanomaterials are currently unavailable, we anyhow chose to follow OECD TG 439, even though it has been validated only for chemicals. However, some limitations can be expected for the testing of nanomaterials. For instance, as for other nanomaterials, GBMs are reported to induce unspecific interactions with the MTT reagent.[9] Hence, as a first step of the research, we evaluated this possibility. OECD TG 439 already considers this potential event suggesting, as a preliminary control check, the evaluation of MTT unspecific reduction induced by the test substance in "killed" RhE tissue. In this manner, the "killed" RhE being not viable, the resulting O.D. signal, if any, can be given only by an unspecific interaction between the test substance and the MTT reagent. However, our results show no unspecific MTT reduction since the O.D. values recorded in GBM-exposed killed RhE were not significantly different from the negative controls (killed RhE not exposed to GBMs). This result is probably due to the barrier property of RhE tissues that do not allow GBMs, added on the top of the RhE surface, to pass into the compartment

below the RhE tissue in which culture medium and/or the MTT reagent are added. To further exclude any interference between GBMs and the MTT reagent, culture media collected from the lower compartments after RhE exposure to GBMs were exposed to the MTT reagent. Also in this case, no increase of the O.D. values was recorded, strengthening the hypothesis reported above. On the whole, these results demonstrate the suitability of the OCED TG 439 to assess GBM irritant potential, considering the MTT assay as a final readout.

The application of OECD TG 439 demonstrates that among the tested GBMs (FLG, FLG-SDS, FLG-SDBS, CVD-graphene, GO and rGO), only FLG exfoliated with SDS and SDBS can be considered as irritant materials. In fact, the resulting RhE viabilities (15 and 35%, respectively) were significantly lower than the threshold given by OECD TG 439 (50% RhE viability). In contrast, none of the other GBMs were able to reduce RhE viability under the OECD threshold. Of particular interest is the effect of FLG-SDS and FLG-SDBS on RhE viability, significantly higher than that of FLG. This result may be due to the higher residues of surfactants in the former materials (36.6 and 38.5%, respectively), used for their exfoliation, as compared to FLG (0.8%). This observation suggests that the irritant properties of FLG-SDS and FLG-SDBS can be related to the presence of residual irritant surfactants after the exfoliation procedure, which are necessary to maintain a stable dispersion of these GBMs. In contrast, FLG, exfoliated using a barely toxic agent such as melamine, turned out to be a non-irritant material, suggesting that the use of non-toxic exfoliation agents may improve GBM safety.

In line with these observations, histological analysis confirmed the absence of signs of irritation for all the GBMs, except for FLG-SDS and FLG-SDBS. Both FLG-SDS and FLG-SDBS induced tissue alterations compatible with skin irritation, such as loss of *stratum corneum* density and disarrangement of the *stratum corneum* and *stratum granulosum* as well as nuclear alterations of keratinocytes of the *stratum basale*. Intriguingly, these alterations are similar to those observed in RhE exposed to the positive controls SDS and SDBS, further supporting the fact that the tissue changes are exerted by the surfactant residues in FLG-SDS and FLG-SDBS. Histological analysis also highlighted the presence of aggregated/agglomerated GBMs (except for GO and CVD-graphene) above the epidermis surface. Also in this case, of particular interest are the results achieved with FLG materials, showing small flat aggregates/agglomerates for FLG and larger ones for FLG-SDS and FLG-SDBS. This different behavior may be related to the different physicochemical properties of these materials, FLG being characterized by an average lateral dimension far smaller than that of FLG-SDS and FLG-SDBS. Intriguingly, GBM depots (except for CVD-graphene), far smaller than the aggregates/agglomerates observed above the epidermis surface, were observed only within the RhE *stratum corneum*. This result suggests that highly dispersed not-aggregated/agglomerated materials could penetrate into the *stratum corneum* but could be not able to pass through the *stratum granulosum* down to the *stratum spinosum* and *stratum basale*. The *stratum corneum* being composed of completely keratinized keratinocytes, the absence of toxicity observed for all the materials, except for FLG-SDS and FLG-SDBS, can be explained by the inability of these materials to deeply penetrate into the inner layers of the epidermis and, therefore, that these materials are unable to directly interact with proliferating keratinocytes of the *stratum basale*. Once again, this observation supports the hypothesis that the toxicity observed for FLG-SDS and FLG-SDBS may be induced by the surfactants rather than by GBMs themselves. In addition, the inability of GBMs to reach the *stratum basale* may explain the apparent discrepancy between these results and those previously obtained on HaCaT skin keratinocytes, at least for FLG and GO, that induced significant cytotoxicity at high concentrations.[11–13] Indeed, HaCaT cells are a simplified model of proliferating keratinocytes more compliant with those typical of the *stratum basale*.

The conclusions based on the evaluation of RhE viability and histological analysis are confirmed by the measurement of IL-1α released by RhE, assessed as a complementary endpoint. Indeed, in 2007, the ECVAM stated that, even though the accuracy of irritant classification is not improved by measuring IL-1α release, this endpoint may be useful to better classify the mild to moderate irritancy potential of a test substance.[23] Accordingly, irritant treatments, either with SDS or SDBS, significantly increase IL-1α release, in line with literature data.[23–27] More importantly, FLG-SDS and FLG-SDBS induced a significant release of IL-1α, at levels comparable to those released by the relevant positive controls. This observation strengthens the conclusion that these materials can be considered as skin irritants and further supports the hypothesis that, for these materials, skin irritation may be due to the surfactant residues. In contrast, none of the other GBMs provoked IL-1α release, corroborating the conclusion that they are not skin irritants. As a further step of the analysis, we focused on two major pro-inflammatory cytokines significantly involved in the modulation of skin inflammation: IL-6 and IL-8.[28,29] In line with the results reported above, a slight but significant release of IL-6 and IL-8 was observed only for FLG-SDS and FLG-SDBS. Of particular interest is the finding that only these materials induced a significant IL-6 release, whereas no effect was exerted by each surfactant alone. This could lead to speculation that the irritation properties of SDS and SDBS residues in FLG-SDS and FLG-SDBS could increase the pro-inflammatory effect of these two materials, by means of IL-6 and IL-8 release. Furthermore, the significant increase of the pro-inflammatory IL-6 and of the chemoattractant IL-8 induced by FLG-SDS and FLG-SDBS cannot exclude a secondary involvement of immune-competent cells, which could further modulate skin inflammation. In this view, previous studies on GBMs showed their ability to upregulate genes implicated in immune responses as well as to induce the release of pro-inflammatory cytokines from peripheral blood mononuclear cells.[30] In addition, GO was able to activate the inflammasome in macrophages[31] and to induce inflammatory cytokine release.[32] Hence, to some extent, these results suggest that the tested GBMs could induce not only an irritant effect, but also an

inflammatory reaction. Nevertheless, the slight increase of IL-6 and IL-8 (far lower than the induced release of IL-1α) cannot directly support this hypothesis.

On the whole, using a non-animal model and OECD guideline, the results of this study demonstrate that exposure of a 3D reconstructed epidermis to GBMs characterized by very low residues of irritant surfactants does not induce any signs of skin irritation. However, it is well known that graphene dispersions are not stable in water after the typical exfoliation treatment (sonication and centrifugation).[33] Thus, a stabilizing agent (surfactants among others) is necessary to avoid the precipitation of the exfoliated graphene. FLG-SDS and FLG-SDBS used in our study were prepared with an amount of surfactants sufficient to allow a stable GBM dispersion (0.05 mg mL^{-1}). Indeed, Coleman and co-workers reported that exfoliation with low concentrations of surfactants (*i.e.*, 0.1 mg mL^{-1} of SDS or SDBS) allows stable dispersions of graphene in water at least for 7 days.[34] A subsequent study demonstrated that the lowest concentration of SDBS allowing the exfoliation and stabilization of graphene in water was equal to 0.05 mg mL^{-1}.[35] Anyway, since in our model GBMs were topically applied on the RhE surface as powder, stable water dispersion of these materials did not represent a limitation. For this reason, to demonstrate the role of surfactant residues in the irritation potential of FLG-SDS and FLG-SDBS, as a final step of the study both materials were further washed after the exfoliation process to reduce the amount of surfactants (0.22% and 1.90%, respectively). These "washed" materials turned out to be non-irritant as assessed by OECD TG 439, by histological analysis as well as by means of cytokine release, as additional endpoints. This result confirmed the hypothesis that the irritation potential of these materials is due to the surfactant residues in the final material rather than to the graphene material itself.

Conclusions

This study was carried out with the aim to investigate the irritation potential of a panel of GBMs using the Reconstructed human Epidermis, a predictive *in vitro* 3D model, approved as an acute non-animal test for skin irritation.

Since no specific guidelines for the testing of nanomaterials at the skin level are currently available, this study was carried out on OECD TG 439, even though it has been validated only for chemicals. As an initial step of the study, we demonstrated that this guideline could be used also for GBMs, at least considering the MTT reduction as a final readout. In fact, no interactions between materials and the MTT reagent were found. In addition, the application of GBMs as powder not only mimics a normal cutaneous exposure, but also avoids any interference due to a serum-dependent protein corona formation, commonly observed in *in vitro* experiments, in which GBMs are suspended in a culture medium containing serum,[36] at the basis of possible underestimation of the *in vitro* effects.

Considering the threshold given by OECD TG 439, the tested GBMs can be considered as non-irritant materials if they contain very low amounts of irritant surfactant residues. However, being nanomaterials and not chemical compounds with defined structures, this result should be considered with care. Indeed, several physicochemical properties (*i.e.* lateral dimension, shape, size, agglomeration state, number of layers, *etc.*) together with the chemical composition may affect the irritant response. To be sure that any irritant properties can be detected, additional analyses were carried out (*i.e.* histological analysis and cytokines release) to implement the OECD guideline. These analyses corroborated the results obtained evaluating RhE viability, confirming that GBMs prepared with irritant surfactants (*i.e.* FLG-SDS and FLG-SDBS) can be considered as irritant materials. On the basis of these observations, we suggest to add these analyses, together with a careful check of any interference with the MTT assay, whenever a nanomaterial is tested following this OECD guideline.

On the whole, these results demonstrate that GBMs characterized by very low amounts of irritant surfactant residues do not seem to induce skin irritation after a single acute exposure. However, since the presence of surfactants is necessary to maintain a stable dispersion of GBMs, these results suggest that the use of non-irritant exfoliation agents (*i.e.* melamine) should be preferred for GBMs designed for biological applications. These results provide a step forward to define GBMs' occupational safety as well as their safe use in devices directly applied to the skin, suggesting that the use of non-toxic surfactants as exfoliation agents may improve their safety.

Author contributions

LF and MP carried out the irritation analysis. MG, CM and EV prepared and characterized FLG materials. AC, BA and AZ prepared and characterized GO, rGO and CVD-graphene materials. MP and CP carried out histological analysis. MP, SS and AT defined the experimental design. AT and MP supervised the study. MP, AT, SS and MP wrote the manuscript.

Conflicts of interest

There are no conflicts to declare.

Acknowledgements

This study was supported by the European Commission funded Graphene Flagship (grant agreement no. 696656, and 785219), the Spanish Ministerio de Economía y Competitividad (project CTQ2017-88158-R and CTQ2016-76721-R), the University of Trieste, and Consorzio Interuniversitario Nazionale per la Scienza e Tecnologia dei Materiali (INSTM). MP, as the recipient of the AXA Chair, is grateful to the AXA Research Fund for financial support. Part of this work was performed under the Maria de Maeztu Units of Excellence Program from the Spanish State Research Agency – Grant No. MDM-2017-0720.

References

1 A. K. Geim and K. S. Novoselov, *Nat. Mater.*, 2007, **6**, 183–191.
2 X. Guo and N. Mei, *J. Food Drug Anal.*, 2014, **22**, 105–115.
3 J. Kim, J. Lee, D. Son, M. K. Choi and D. H. Kim, *Nano Convergence*, 2016, **3**, 4.
4 S. R. Shin, Y. C. Li, H. L. Jang, P. Khoshakhlagh, M. Akbari, A. Nasajpour, Y. S. Zhang, A. Tamayol and A. Khademhosseini, *Adv. Drug Delivery Rev.*, 2016, **105**, 255–274.
5 M. V. D. Z. Park, E. A. J. Bleeker, W. Brand, F. R. Cassee, M. van Elk, I. Gosens, W. H. de Jong, J. A. J. Meesters, W. J. G. M. Peijnenburg, J. T. K. Quik, R. J. Vandebriel and A. J. A. M. Sips, *ACS Nano*, 2017, **11**, 9574–9593.
6 M. Pelin, S. Sosa, M. Prato and A. Tubaro, *Nanoscale*, 2018, **10**, 15894–15903.
7 B. Fadeel, C. Bussy, S. Merino, E. Vázquez, E. Flahaut, F. Mouchet, L. Evariste, L. Gauthier, A. J. Koivisto, U. Vogel, C. Martín, L. G. Delogu, T. Buerki-Thurnherr, P. Wick, D. Beloin-Saint-Pierre, R. Hischier, M. Pelin, F. Candotto Carniel, M. Tretiach, F. Cesca, F. Benfenati, D. Scaini, L. Ballerini, K. Kostarelos, M. Prato and A. Bianco, *ACS Nano*, 2018, **12**, 10582–10620.
8 C. Klaassen, *Casarett & Doull's Toxicology: the basic science of poisons*, McGraw-Hill, Health Professions Division, New York, 2013.
9 K. H. Liao, Y. S. Lin, C. W. Macosko and C. L. Haynes, *ACS Appl. Mater. Interfaces*, 2011, **3**, 2607–2615.
10 Y. Li, H. Yuan, A. von dem Bussche, M. Creighton, R. H. Hurt, A. B. Kane and H. Gao, *Proc. Natl. Acad. Sci. U. S. A.*, 2013, **110**, 12295–12300.
11 M. Pelin, L. Fusco, V. León, C. Martín, A. Criado, S. Sosa, E. Vázquez, A. Tubaro and M. Prato, *Sci. Rep.*, 2017, **7**, 40572.
12 M. Pelin, L. Fusco, C. Martín, S. Sosa, J. Frontiñan-Rubio, J. M. Gonzalez-Dominguez, M. Duran, E. Vázquez, M. Prato and A. Tubaro, *Nanoscale*, 2018, **10**, 11820–11830.
13 J. Frontiñán-Rubio, M. V. Gómez, C. Martín, J. M. González-Domínguez, M. Durán-Prado and E. Vázquez, *Nanoscale*, 2018, **10**, 11604–11615.
14 V. León, M. Quintana, M. A. Herrero, J. L. Fierro, A. de la Hoz, M. Prato and E. Vázquez, *Chem. Commun.*, 2011, **47**, 10936–10938.
15 V. León, A. M. Rodriguez, P. Prieto, M. Prato and E. Vázquez, *ACS Nano*, 2014, **8**, 563–571.
16 V. León, J. M. González-Domínguez, J. L. Fierro, M. Prato and E. Vázquez, *Nanoscale*, 2016, **8**, 14548–14555.
17 J. M. González-Domínguez, V. León, M. I. Lucío, M. Prato and E. Vázquez, *Nat. Protoc.*, 2018, **13**, 495–506.
18 U. Mogera, R. Dhanya, R. Pujar, C. Narayana and G. U. Kulkarni, *J. Phys. Chem. Lett.*, 2015, **6**, 4437–4443.
19 A. C. Ferrari, J. C. Meyer, V. Scardaci, C. Casiraghi, M. Lazzeri, F. Mauri, S. Piscanec, D. Jiang, K. S. Novoselov, S. Roth and A. K. Geim, *Phys. Rev. Lett.*, 2006, **97**, 187401.
20 K. R. Paton, E. Varrla, C. Backes, R. J. Smith, U. Khan, A. O'Neill, C. Boland, M. Lotya, O. M. Istrate, P. King, T. Higgins, S. Barwich, P. May, P. Puczkarski, I. Ahmed, M. Moebius, H. Pettersson, E. Long, J. Coelho, S. E. O'Brien, E. K. McGuire, B. M. Sanchez, G. S. Duesberg, N. McEvoy, T. J. Pennycook, C. Downing, A. Crossley, V. Nicolosi and J. N. Coleman, *Nat. Mater.*, 2014, **13**, 624–630.
21 F. Torrisi, T. Hasan, W. Wu, Z. Sun, A. Lombardo, T. S. Kulmala, G. W. Hsieh, S. Jung, F. Bonaccorso, P. J. Paul, D. Chu and A. C. Ferrari, *ACS Nano*, 2012, **6**, 2992–3006.
22 C. Tornier, C. Amsellem, B. Fraissinette Ade and N. Alépée, *Toxicol. in Vitro*, 2010, **24**, 245–256.
23 C. Pellevoisin, C. Videau, D. Briotet, C. Grégoire, C. Tornier, A. Alonso, A. S. Rigaudeau, C. Bouez and N. Seyler, *Toxicol. in Vitro*, 2018, **50**, 418–425.
24 J. Choi, H. Kim, J. Choi, S. M. Oh, J. Park and K. Park, *Environ. Health Toxicol.*, 2014, **29**, e2014004.
25 M. Niwa, K. Nagai, H. Oike and M. Kobori, *Biol. Pharm. Bull.*, 2009, **32**, 203–208.
26 D. S. Olsen, M. Lee and A. P. Turley, *Toxicol. in Vitro*, 2018, **50**, 426–432.
27 S. W. Spiekstra, M. J. Toebak, S. Sampat-Sardjoepersad, P. J. van Beek, D. M. Boorsma, T. J. Stoof, B. M. von Blomberg, R. J. Scheper, D. P. Bruynzeel, T. Rustemeyer and S. Gibbs, *Exp. Dermatol.*, 2005, **14**, 109–116.
28 M. D. Turner, B. Nedjai, T. Hurst and D. J. Pennington, *Biochim. Biophys. Acta*, 2014, **1843**, 2563–2582.
29 B. Nedoszytko, M. Sokołowska-Wojdyło, K. Ruckemann-Dziurdzińska, J. Roszkiewicz and R. J. Nowicki, *Postepy Dermatol. Alergol.*, 2014, **31**, 84–91.
30 M. Orecchioni, D. Bedognetti, L. Newman, C. Fuoco, F. Spada, W. Hendrickx, F. M. Marincola, F. Sgarrella, A. F. Rodrigues, C. Ménard-Moyon, G. Cesareni, K. Kostarelos, A. Bianco and L. G. Delogu, *Nat. Commun.*, 2017, **8**, 1109.
31 S. P. Mukherjee, K. Kostarelos and B. Fadeel, *Adv. Healthcare Mater.*, 2018, **7**, 1700815.
32 J. Ma, R. Liu, X. Wang, Q. Liu, Y. Chen, R. P. Valle, Y. Y. Zuo, T. Xia and S. Liu, *ACS Nano*, 2015, **9**, 10498–10515.
33 S. Barwich, U. Khan and J. N. Coleman, *J. Phys. Chem. C*, 2013, **117**, 19212–19218.
34 R. J. Smith, M. Lotya and J. N. Coleman, *New J. Phys.*, 2010, **12**, 125008.
35 S. Wang, M. Yi and Z. Shen, *RSC Adv.*, 2016, **6**, 56705–56710.
36 S. P. Mukherjee, M. Bottini and B. Fadeel, *Front. Immunol.*, 2017, **8**, 673.